


Article

Ring Shape Microstrip Antenna Backed by Modified Ground Plane for Multiband Response in GSM and Radar Applications

Aarti G. Ambekar¹ , Amit A. Deshmukh¹ 

¹ *Electronics and Telecommunication Department, D J Sanghvi College of Engineering, Mumbai, Maharashtra India. arti1910@gmail.com, amitdeshmukh76@gmail.com*

Abstract— Ring shape microstrip antenna designs supported via an altered ground plane profile are proposed for multi-band response with wider bandwidth in each band. The impedance bandwidth of a single ring patch supported via a slot cut ground plane on a substrate having a thickness of $\sim 0.1\lambda_g$, is 45.8% and the broadside gain is 5.6 dBi. By employing additional stack patches, dual and triple-band configurations are obtained. In the respective operative frequency bands, maximum 15% of bandwidth is achieved in the suggested antenna, with a maximum broadside gain of more than 5.5 dBi. Through the acquired antenna features, the proposed configuration fulfills the criteria of E-GSM900/Secondary Surveillance Radar/Aeronautical Radio Navigation Applications.

Index Terms— Modified ground plane, Proximity feed, Rectangular slot, Ring shape microstrip antenna

I. INTRODUCTION

In recent decades, technologies based on wireless communication have grown in popularity and demand. Designing a multiband antenna is crucial to satisfy the demands for frequency agility of contemporary wireless technologies. Microstrip antenna (MSA) are notably in demand in the modern communication system despite their low bandwidth (BW) and gain, but owing to their compact profile, lightweight, besides simplicity of system integration [1] – [4]. A number of methods, such as the use of an electrically thicker substrate, parasitic patches, and altered patch geometry in the form of slots or stubs, can be employed to provide a multiband response that offers BW enhancement [1] – [4]. The slot cut approach is employed as it offers compactness [5] – [6], whereas tuning stubs are favored for frequency tuning [7]. The achieved BW is lower in the multiband designs stated in [8] – [9] despite being built on an electrically thicker substrate. Artificial magnetic conductors or meta-surfaces are employed for gain enhancement in [10] – [12]. The technique reported here increases the configuration's overall cost and the complexity. Owing to the fractal geometry, the complexity of the structure increases for a multi wide band antenna reported in [13]. With the inclusion of biasing circuits, reconfigurable designs incorporating active devices make the implementation complex [14] – [16]. For the realization of penta-band response, slots, and stubs are used in [17]. The defected ground plane structure and slots are used to obtain dual-band response in [18], [24]. The combination of slots, stubs, and shorting posts is used for tuning multiband response in [19] – [23]. All these reported

configurations do not cover in detail how the modifications incorporated in the main patch or the ground plane alter the input impedance and the resonance frequency at patch resonant modes, to yield the multiple frequencies.

Proximity-fed ring shape MSA variations on air-suspended FR4 substrate, covering a frequency range of 1000 MHz, are presented in this paper. Initially, the offset proximity-fed design of a basic circular ring patch is discussed that yields an impedance BW of 128 MHz (10%). Further, a combination of defects on the ground plane in the form of rectangular slots and vertical stub on the patch yields an optimum separation between the degenerated fundamental modes of the ring patch (TM_{01d} and TM_{01v}) that gives a wider impedance BW of 534 MHz (45.8%), offering broadside gain of more than 5 dBi. Electromagnetically coupled stacked variations of proximity-fed stub loaded ring shape MSAs with a ring shape MSA or stub loaded ring shape MSA are proposed, which yields dual-band or triple-band response, offering a frequency agility. The optimum dual-band antenna employing a stacked ring patch covers two frequency bands: 970 MHz and 1267 MHz with respective BW of 16.9% and 18.3% and broadside gain of 5.7 and 4.6 dBi, individually. The triple band antenna, employing stub loaded stacked ring MSA, covers frequency bands of 1002 MHz, 1125 MHz, and 1322 MHz with a respective BW of 16.5%, 6.9%, and 7.1% and a broadside gain of 5.4, 4.8, and 3.2 dBi respectively. All configurations exhibit a broadside radiation pattern. Projected multi-band configurations yields a frequency agility fulfilling the criteria for E-GSM900/Secondary surveillance radar/aeronautical radio navigation applications.

The uniqueness of the present investigation is in the detailed explanation of recognition of multi-band response with a wider BW in each band through the analysis of the degenerated resonant mode excitation in proximity-fed ring shape MSA. The proposed design is easier to fabricate and provides a noticeable gain and BW compared to the reported multiband MSAs that have a BW of over 5% in each band. Further closely spaced frequency bands are observed with bearing ratios of 1:1.3 and 1:1.12:1.31, in dual band and triple band configurations. The paper continues with a thorough comparison stressing the innovative aspects of the suggested investigation. Initial IE3D simulations [25] are used to optimize the configurations revealed in this paper, then the measurements are taken. The ring shape MSA is excited using a 50 Ω SMA connector of 0.12 cm inner wire diameter. Within the antenna laboratory, utilizing high-end instruments like ZVH-8, FSC 6, and SMB 100A, the simulation results' experimental validation for input impedance, radiation pattern and gain has been completed. Setting up for more precise measurement, it employs the three-antenna gain approach to evaluate gain in a laboratory. The findings of simulations and measurements show high agreement.

II. STUB LOADED RING SHAPE MSA BACKED BY RECTANGULAR SLOTS CUT GROUND PLANE

A more compact version of circular MSA (CMSA) is the circular ring-shape MSA and it is derived by cutting a circular slot in the patch center [4]. A variation of the electromagnetic feeding technique, proximity feeding achieves an improvement in MSA BW on a thicker substrate [3] – [4]. Using the

same, the design of circular ring MSA supported by rectangular slots cut ground plane is proposed as revealed in Fig. 1(a), Fig. 1 (b). In proximity feeding, fringing fields from the coupling strip are coupled to the radiating patch that excites the resonant mode in the ring shape antenna.

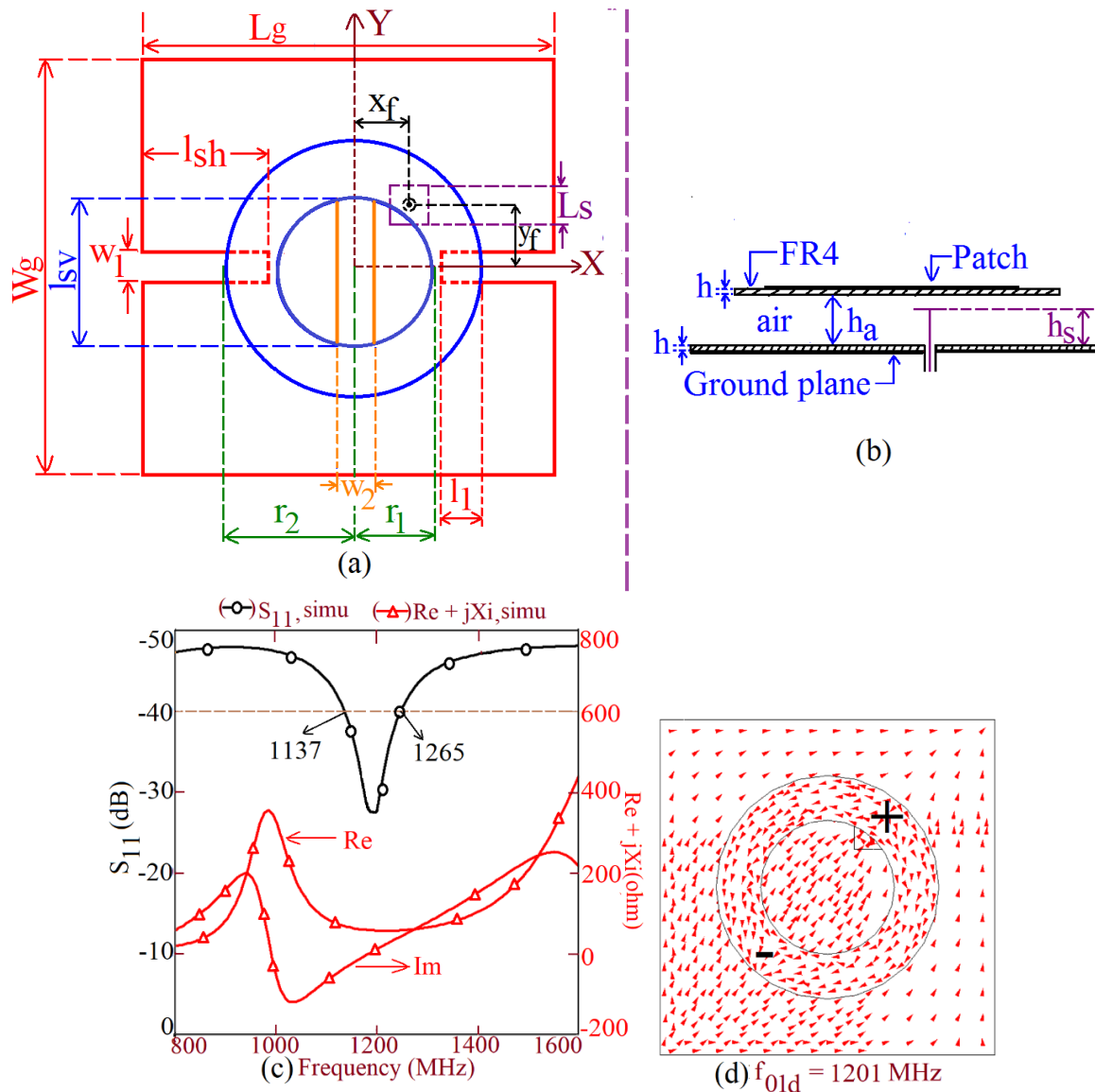


Fig. 1 (a) Top and (b) side views, (c) simulated reflection coefficient (S_{11}) & resonance curve plots, and (d) surface current distributions for the offset proximity fed circular ring MSA

A thicker substrate suspended design is chosen, comprising of two FR4 substrate layers ($\epsilon_r = 4.3$, $h = 0.16$ cm), separated by a h_a cm air gap. The paper refers to the patch dimensions and frequencies in ‘cm’ and ‘MHz’ respectively. To achieve the fundamental mode frequency of 1000 MHz in ring MSA, for $h_a = 2.8$ cm, $h_s = 2.6$ cm, $L_s = 1.6$ cm and ground plane dimensions as, $L_g = W_g = 16$ cm, the ring patch dimensions are parametrically calculated using IE3D simulations as $r_2 = 5$ & $r_1 = 3.0$ cm. At the fundamental resonant mode, MSA shows a broadside radiation pattern. The present study aims at realizing multi-band antenna to offer a broadside pattern in each band. For broadside patterns across each band, variations of fundamental mode are only needed and this is possible by realizing the

degeneration of the fundamental mode. Hence initially the ring MSA is fed at an offset feed position, i.e. at $x_f, y_f = 2.0, 2.5$ cm, as shown in Fig. 1(a). As seen from the provided simulated results in Fig. 1(c), with offset feed position also, a single peak in the resonance curve is noted and MSA shows an impedance BW of 128 MHz (10%). According to the surface current circulation at the corresponding resonant peak in Fig. 1(d), there is a half-wavelength variation around the patch's diameter besides a diagonal variation in 45° directions. Owing to this variation, the resonant mode is stated as TM_{01d} mode. The 'd' refers to the diagonal variation. To further explore the degeneration of the fundamental mode, perturbation in current components at TM_{01d} mode is needed. For this modification in the ground plane is considered. The current perturbation can be achieved by placing a slit or stub on the patch, but this affects the shape of the geometry. Hence ground plane slot is selected. As depicted in Fig. 1(a), two rectangular slots, each measuring length l_{sh} and width w_1 , are embedded along the ground plane's width. The slot is oriented on the ring patch so that its length is orthogonal to the currents in TM_{01d} mode. A parametric analysis of the effects of ground plane slots is conducted. Fig. 2(a) displays resonance curve plots for two slot lengths. When the ring patch is covered by the slot length l_{sh} ($l_1 = 2.0$ cm), then degeneration of fundamental mode is noted.

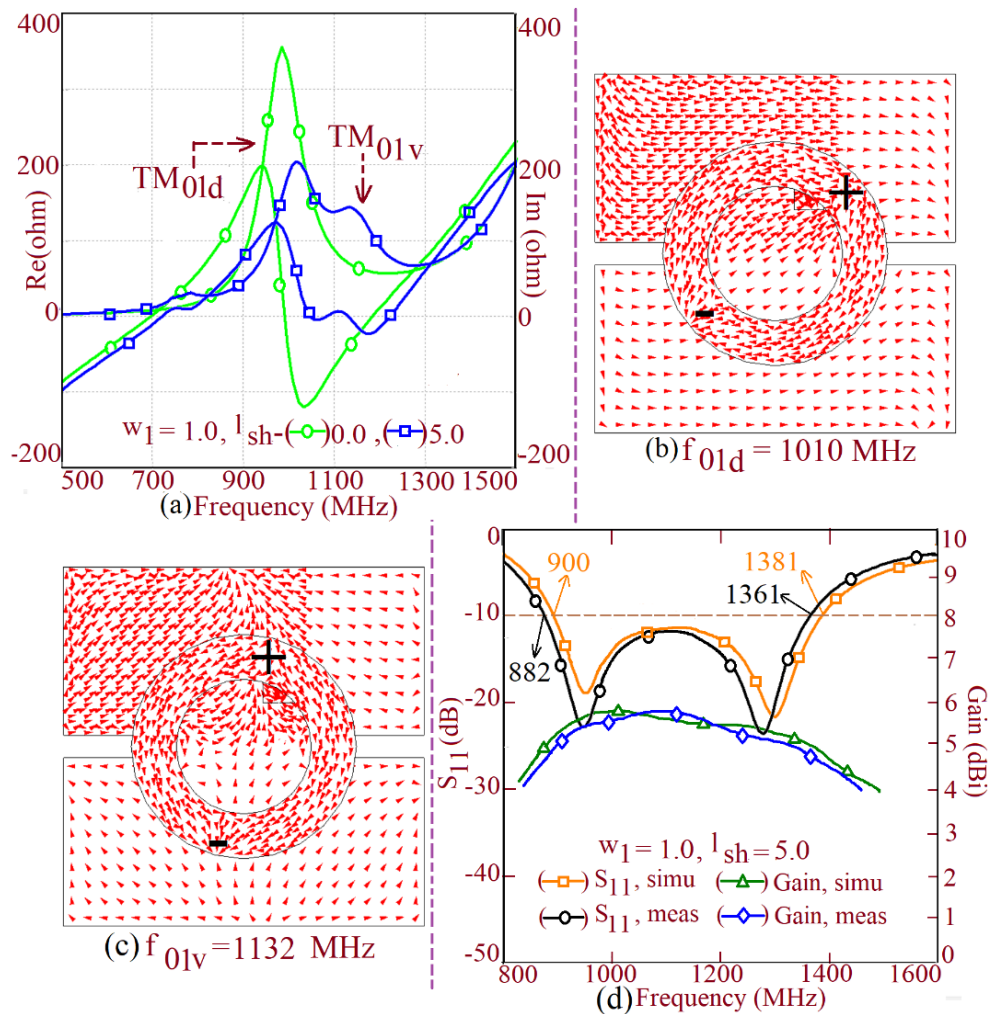


Fig. 2 (a) Resonance curve plots for ground plane slot length variation, (b, c) surface current distribution at the two degenerated modes, and (d) S_{11} BW and gain plots for circular ring MSA backed by slots cut ground plane

Fig. 2(b), Fig. 2(c) displays surface current distributions at degenerated modes. The diagonal axis continues to be the path of surface currents in the first mode. Currents in the second mode vary in the vertical direction. With these current variations, respective modes are mentioned as TM_{01d} and TM_{01v} . By optimizing the slot length, optimum spacing between the two modes is obtained. Further, the optimization of the feed location yields maximum BW as depicted in Fig. 2(d). The optimized antenna dimensions are $l_{sh} = 5.0$ cm, $w_1 = 1.0$ cm, $h_a = 2.6$ cm, $h_s = 2.5$ cm, $L_s = 1.0$ cm, $x_f = 1.5$, and $y_f = 2.6$ cm. The simulated and measured BW in circular ring MSA backed by slot cut ground plane is 481 MHz (42.17%) and 479 MHz (42.71%), respectively. Over the whole $S_{11} \leq -10$ dB BW, antenna broadside gain is greater than 5 dBi. Broadside radiation pattern is appearing across the BW with a cross polar level of less than -14 dB as opposed to a co-polar level. The E-plane is aligned along $\Phi = 90^\circ$ over the BW. An increment in the ground plane slot length beyond 5 cm is not considered as it creates a complete slot below the ring patch. The TM_{01d} and TM_{01v} resonant modes are not orthogonal and hence circular ring MSA with slot cut ground yields linear polarized wideband response.

For further increase in BW, tuning of the two modes is needed. In the middle of the ring patch, a stub of length w_2 and width l_{sv} is positioned to accomplish this, as shown in Fig. 1(a). This stub position creates a shorter path length for currents at TM_{01v} mode, which increases its frequency and thus increases the BW as depicted in Fig. 3(a). For $w_2 = 1.5$ cm, $x_f = 1.7$, and $y_f = 2.8$ cm, the construction of a loop inside the $VSWR = 2$ circle produces the finest results. As depicted in Fig. 3(b), the simulated BW is 534 MHz (45.8%) whereas the measured BW is 524 MHz (45.9%). Antenna broadside gain is more than 5 dBi across S_{11} BW. Polar plots in Fig. 3(c)– Fig. 3(f) displays radiation pattern that are closer to the BW's band start and stop frequencies. At frequencies publicized and over the complete BW, the pattern remains in the broadside direction with the E-plane aligned along $\Phi = 90^\circ$. The cross polar radiation is below 8 – 10 dB with respect to co-polar levels. A higher contribution of the cross-polarization level is attributed to the small contribution of horizontal currents due to the diagonal variation of resonant mode currents. The fabricated prototype for the stub loaded circular ring MSA is depicted in Fig 4.

III. ELECTROMAGNETICALLY COUPLED MULTIBAND VARIATIONS OF RING SHAPE MSAS

Multi-band response offering wider BW in each band is obtained when a greater number of resonant modes are present in the configuration. To explore the same, electromagnetically coupled stacked configuration of ring MSAs is considered as shown in Fig. 5(a). With a circular ring geometry, a planar gap-coupled design will not produce the best coupling within fed and parasitic patches owing to the smaller coupling area through a single tangential point which leads to inadequate BW improvement. and hence the stacked design is considered. Two variations of stacked configurations; the first one with ring shape MSA and the second with stub loaded ring shape MSA is

explored. Dimensions among a stub with a width of $w_2 = 1.5$ cm on the stacked patch, as illustrated in Fig. 1(a), the stacked ring MSAs variations are kept the same as that of fed ring MSA, but an air gap among the two patches is altered to tune the respective modal frequencies.

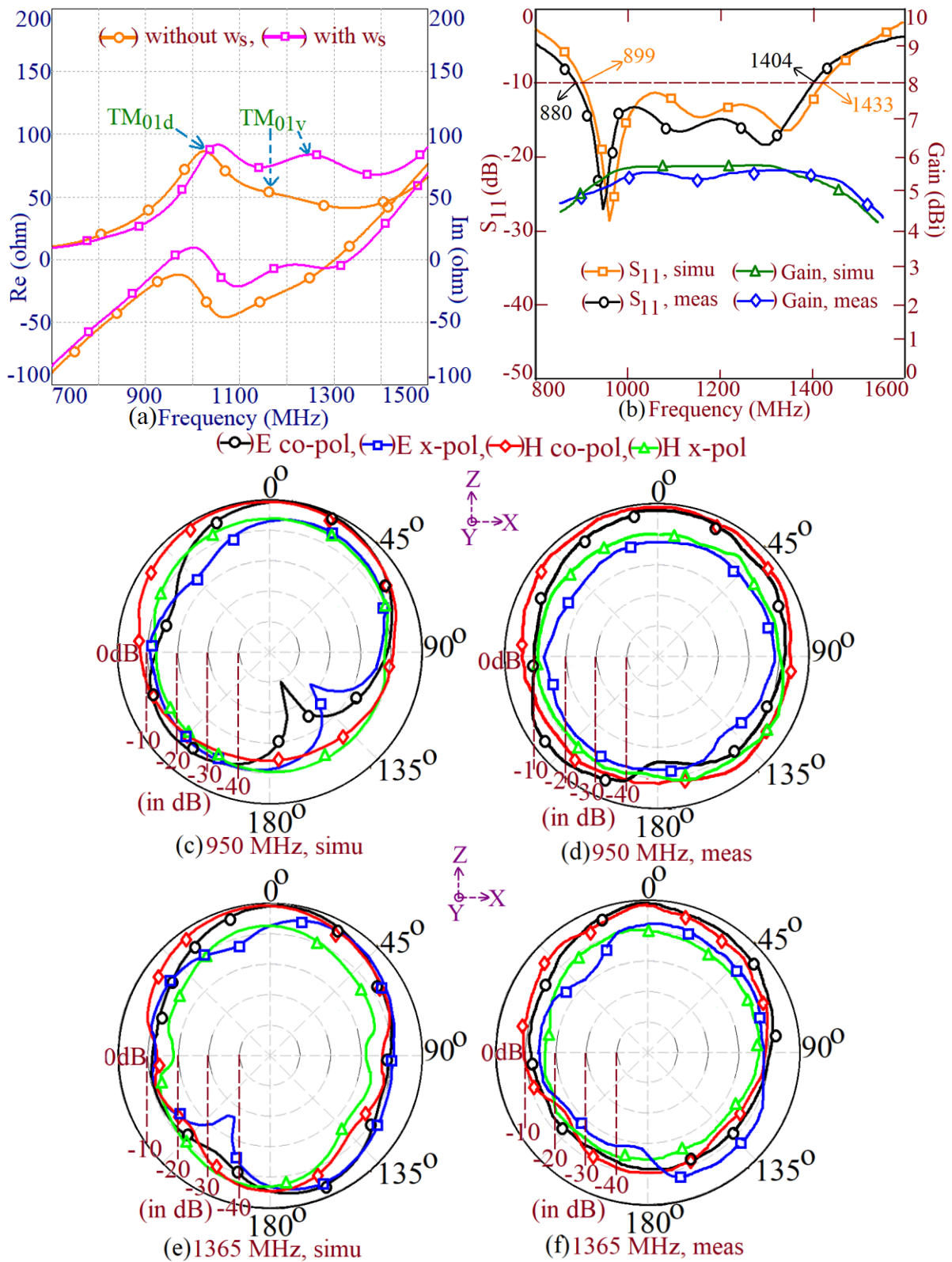


Fig. 3 (a) Resonance curve for circular ring shape MSA with and without stub, (b) S_{11} BW and gain plots, radiation pattern nearer to band (c, d) start and (e, f) stop frequencies of BW for stub loaded circular ring MSA backed by rectangular slots cut ground plane.

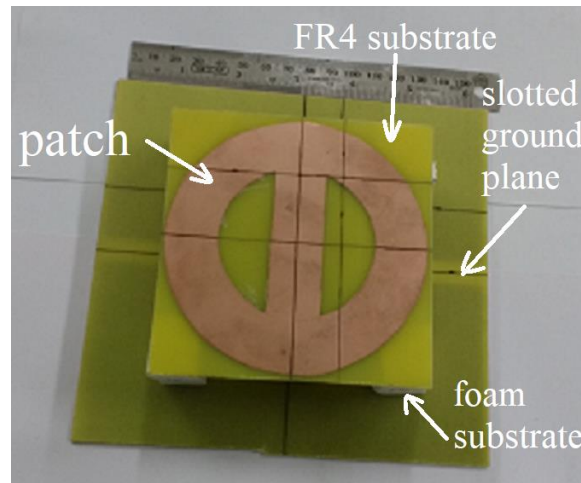


Fig. 4 Fabricated prototype of stub-loaded ring shape MSA backed by slot cut ground plane.

In the two stacked variations, resonance curve plot in Fig. 5(b) displays four peaks. A dual wideband response is observed in the combination of fed stub loaded ring MSA stacked with a ring MSA. As the inter-spacing between the modal frequencies on the ring patches changes with the placement of the stub on the stacked ring MSA, dual band response changes to the triple frequency response with BW greater than 5% in each band, for stub loaded ring patch stacked on the fed stub loaded ring patch. The dimensions of the fed and stacked patches and the air gap between them are parametrically optimized using IE3D simulations for the respective responses. In the dual wideband response, fed patch antenna parameters are, $r_1 = 3$, $r_2 = 5$, $w_2 = 1.5$, $h_a = 2.6$, $h_s = 2.5$, $L_s = 1.0$, $x_f = 1.7$, $y_f = 2.8$ cm. The dimensions of the stacked patch are the same as that of the fed ring MSA, but it is placed at $h_1 = 0.7$ cm above the fed ring MSA. Fig. 6(a) displays the S_{11} BW and gain plots for optimized dual band configuration.

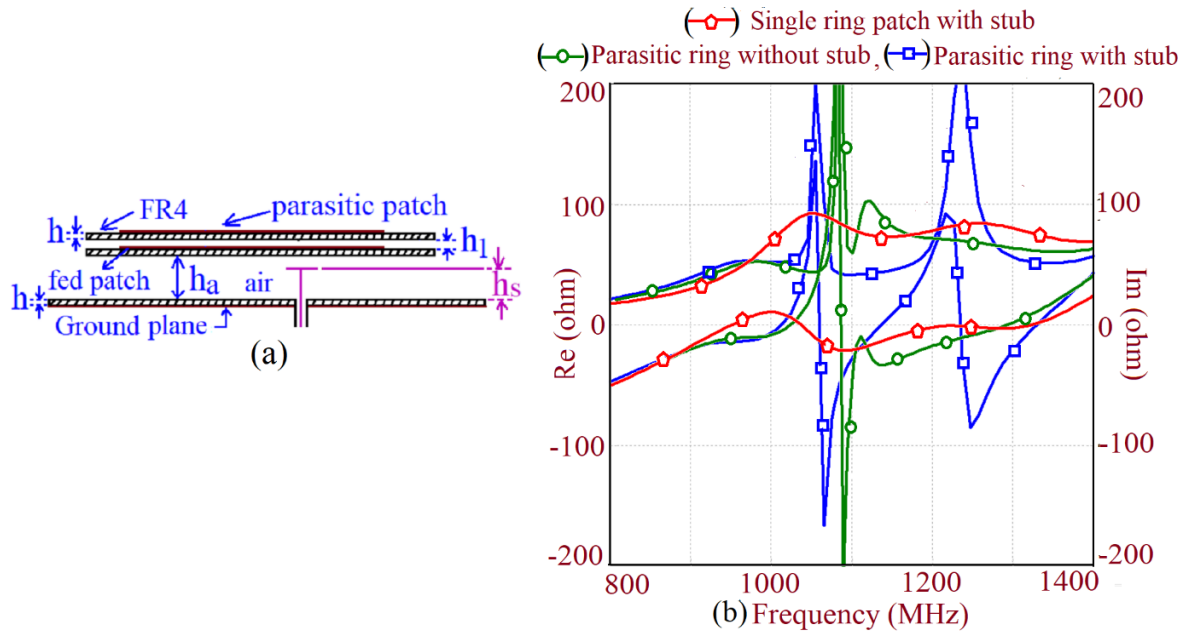
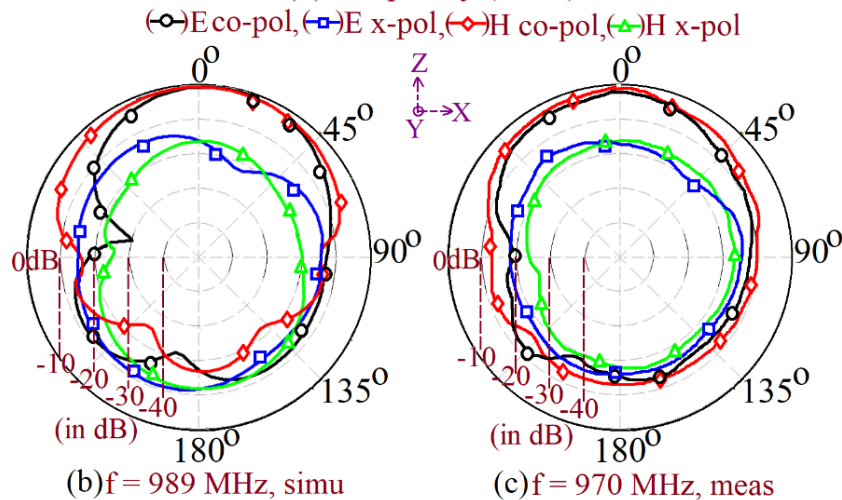
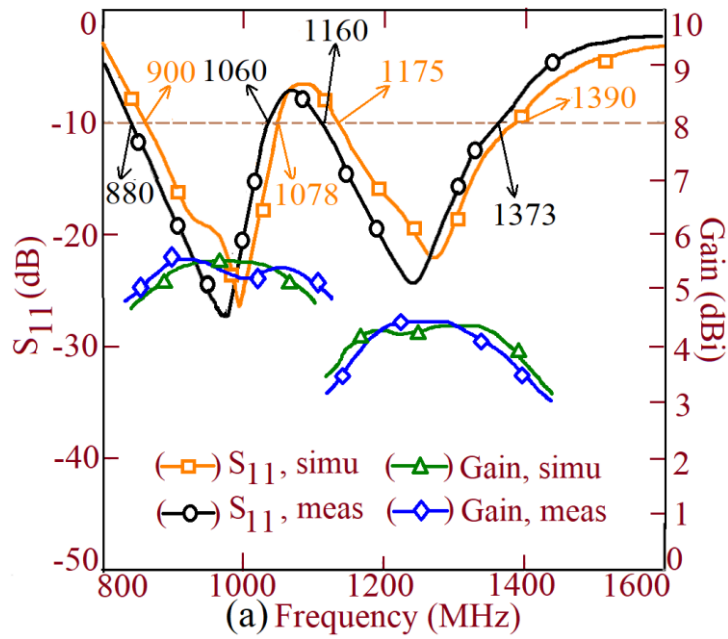


Fig. 5 (a) Side view for multi-layer stacked configuration, (b) overlapped resonance plots for all the variations of the proposed ring shape MSA.



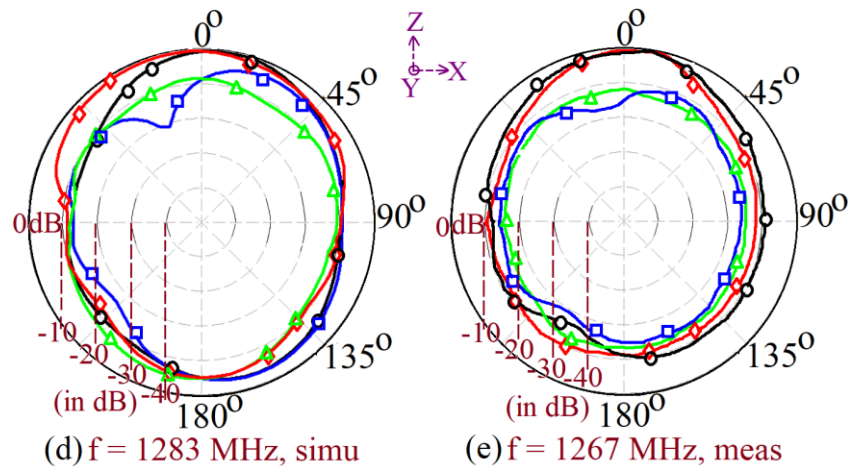


Fig. 6 (a) S_{11} BW and gain plots and radiation patterns at the center frequency of (b, c) first and (d, e) second band for the dual-band stacked ring shape MSAs

Respective simulated impedance BW across the two bands are 178 MHz (16.5%) and 215 MHz (18.2%). While the equivalent measured values are 180 MHz (16.9%) and 213 MHz (18.3%), respectively. Simulated and measured gain across the first band is more than 5 dBi while in the second band, it is above 4 dBi. Fig. 6(b) - Fig. 6(e) displays the radiation patterns at the center frequency of each band. The pattern is broadside-directed and the cross-polar level against the co-polar component of radiation is less than 8 dB. The E-plane of radiation is aligned along $\Phi = 90^\circ$. With the above antenna characteristics, the proposed antenna fulfills the necessities of E-GSM900 (880 – 960 MHz), aeronautical radio service navigation (1164 to 1215 MHz, 1215 -1240 MHz, 1240-1300 MHz, 1300 – 1350 MHz). The fabricated antenna is shown in Fig. 7.

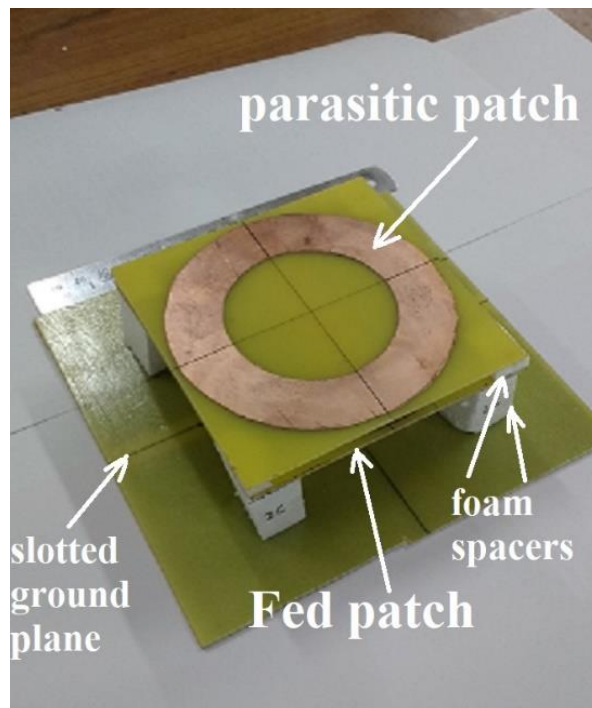
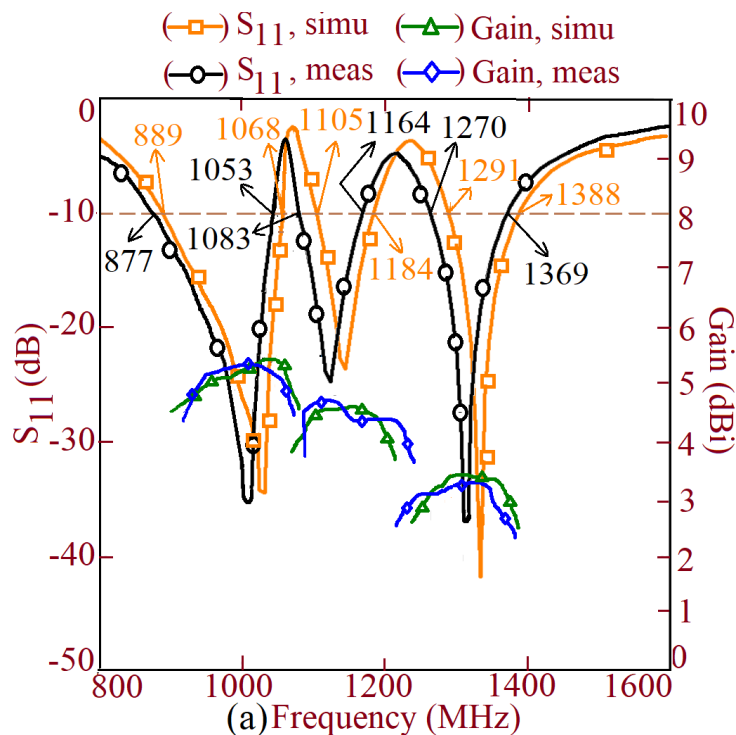


Fig. 7 Fabricated prototype of stacked ring shape MSAs for dual wideband response

A triple frequency response is achieved using the same antenna dimensions as those used in the dual band design and with the positioning of a stub with a width of $w_2 = 1.5$ cm on the stacked patch. Thus, configuration consist of fed stub loaded ring MSA stacked with a stub loaded ring MSA. As shown in Fig. 8(a) the simulated impedance BW across the respective bands are 179 MHz (16.7%), 79 MHz (6.7%), and 97 MHz (6.9%), while the respective measured values are 176 MHz (16.5%), 81 MHz (6.9%), and 99 MHz (7.1%). The simulated and measured gain across the first band is more than 5 dBi while for the second band, it is more than 4 dBi. In the third band gain is more than 3.0 dBi. The three consecutive band center frequencies have a frequency ratio of 1:1.12:1.31. This ratio shows strong frequency agility amongst subsequent bands, which helps prevent channel interference. The simulated and measured radiation patterns observed at the center frequencies of the three bands are shown in Fig. 8(b) – Fig. 8(e) and Fig. 9(a), Fig. 9(b). The pattern in three bands shows maximum in the bore-sight direction with cross polarization level of less than 8 dB against the co-polar level. With this achieved BW, pattern and gain characteristics, the proposed antenna fulfills the necessities of E-GSM900 (880 – 960 MHz) and Secondary surveillance radar (SSR) uplink (1030 MHz) as well as downlink (1090 MHz) frequencies, and service aeronautical radio navigation (1300 – 1350 MHz).



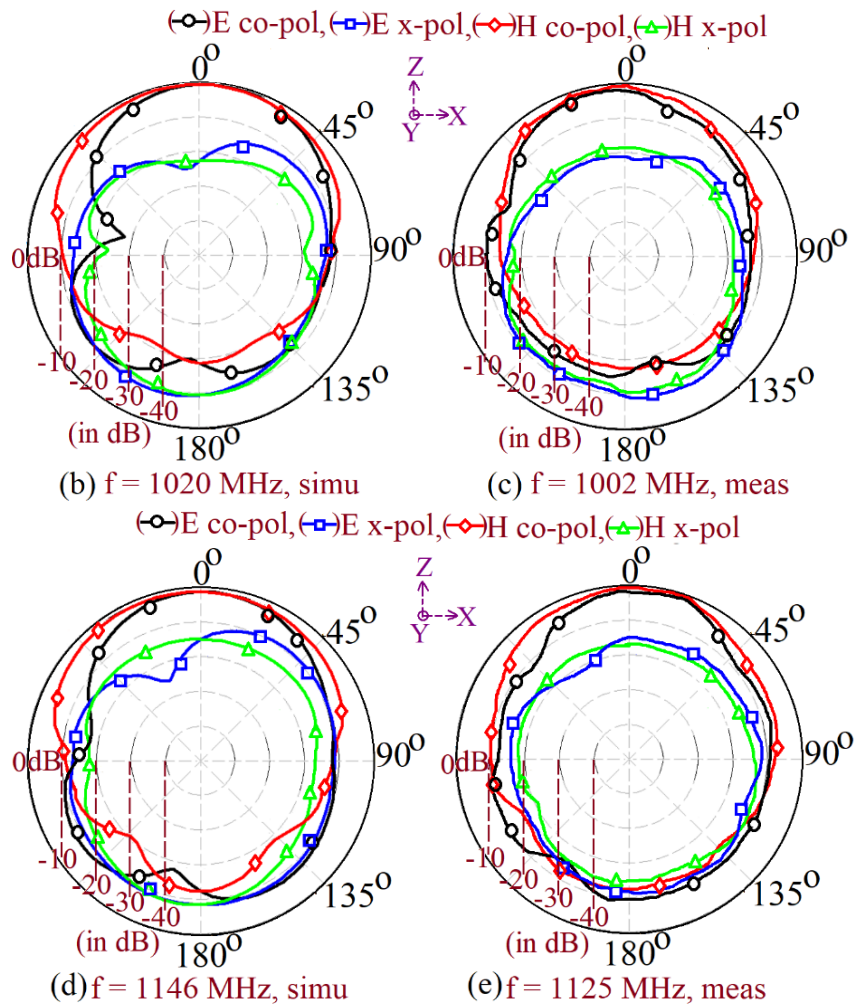
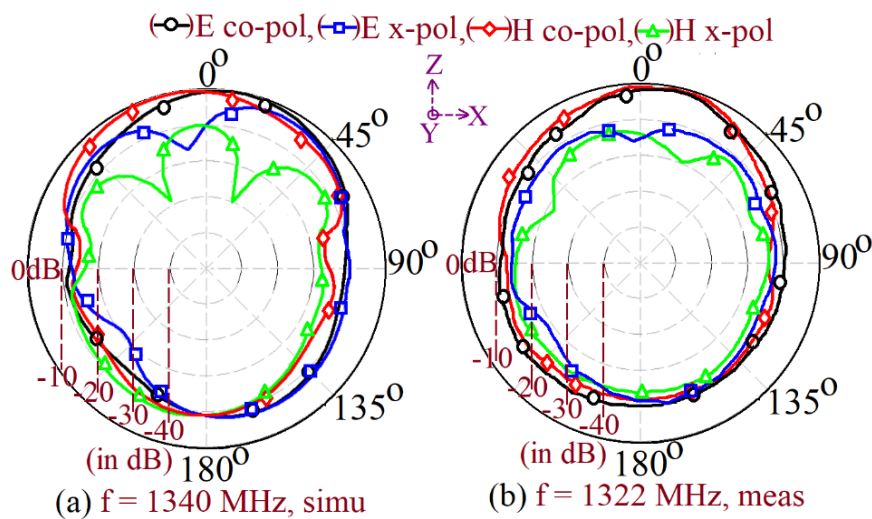


Fig. 8 (a) S_{11} BW and gain plots and (b – e) polar radiation patterns at the center frequency in the first & second bands for triple-band ring shape MSA



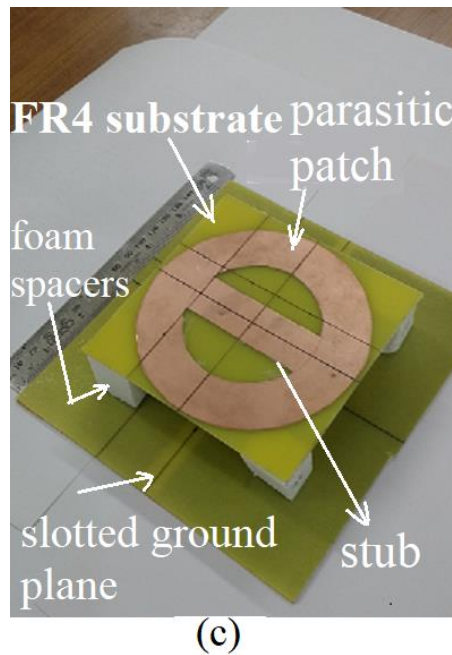


Fig. 9 (a, b) Radiation pattern at the center frequency of the third band and (c) fabricated prototype of ring shape MSA for the triple-band response.

The Fig. 9(c) displays the fabricated prototype for the triple frequency design. In the antenna lab, measurements of the suggested design's input impedance, pattern, and gain are made by means of instruments, ZVH – 8, FSC 6, and SMB 100A. The distinctions in substrate characteristics, air gap, feed point location, and antenna size are what cause the observable differences between the measured and the simulation results.

IV. RESULTS DISCUSSION AND COMPARATIVE ANALYSIS

The paper presents designs of ring shape MSAs for dual and triple frequency response. A comparison of the technical innovation in the proposed study and the findings achieved in stated multi-band MSAs appears in Table I. The comparison is presented based on a number of frequency bands and respective BW, techniques to achieve the said response, peak gain in the respective bands, and the antenna volume, i.e patch area (A_p) and total substrate thickness (h_t).

TABLE I. COMPARISON OF THE PROPOSED MULTIBAND RING SHAPE MSA AGAINST REPORTED PAPER

MSA shown in	fc, BW MHz (%)	Frequency ratio $f_2/f_1, f_3/f_1, f_3/f_2$	Tuning element	Peak Gain (dBi)	$A_p/\lambda_c, h_t/\lambda_c$
Fig. 7	970 (16.9), 1267 (18.3),	1.30	slot, stub	5.7, 4.6	$2.6\lambda_c, 0.1\lambda_c$
Fig. 9(c)	1002 (16.5), 1125 (6.9), 1322 (7.1)	1.12, 1.31, 1.17	slot, stub	5.4, 4.8, 3.2	$2.6\lambda_c, 0.1\lambda_c$
[8]	1300 (3), 1800 (4.3), 2330 (3.5)	1.38, 1.79, 1.29	slot	—	$1.17\lambda_c, 0.06\lambda_c$
[9]	2440 (6.6), 5730 (4.8)	2.36	slot	6.8, 2.1	$1.6\lambda_c, 0.06\lambda_c$
[10]	3360 (-), 5670 (-), 9100 (-)	1.68, 2.70, 1.60	—	3.3, 6.3, 11.7	$6.5\lambda_c, 0.08\lambda_c$
[11]	2400 (1.3), 4200 (42), 5800	1.75, 2.41, 1.38	—	4.2, 1.9,	$2.0\lambda_c,$

	(15)			3.46	0.25 λ_c
[12]	2360 (24), 8450 (10.36)	1.43, 2.14, 1.49	—	2, 4.5	0.53 λ_c , 0.015 λ_c
[13] Antenna-II	3400 (-), 4600 (-), 6000 (-), 8000 (-), 10400 (-), 12400 (-), 13700 (-)	1.35, 1.76, 1.30	—	5.32, 1.84, 0.82, 3.2, 3.4, 5.4, 20.4	1.02 λ_c , 0.014 λ_c
[14] At port 1 diode on	3600 (1.05), 6780 (7.3), 9080 (0.69), 13150 (0.52), 15330 (13.8), 17550 (22)	1.05, 2.52, 2.40	Slot, PIN diode	8	4.4 λ_c , 0.02 λ_c
[15] Triple band	859 (15), 1592 (6.83), 2450 (4.9)	1.85, 2.85, 1.53	PIN diode	—	1.63 λ_c , 0.65 λ_c
[16]	5210 (2.6), 9410 (9.6) 10460 (3.9), 12690 (6.4), 14390 (3.0), 17090 (17)	1.80, 2.0, 1.1	PIN diode	3.96	1.57 λ_c , 0.02 λ_c
[18]	2460 (38), 5100 (13)	2.36	slots	2.5, 4.2	0.2 λ_c , 0.012 λ_c
[21]	2400 (38), 3700 (13)	1.54	—	4.3	0.5 λ_c , 0.012 λ_c
[22]	1900 (4), 3500 (2.2)	1.84	Shorting pins	1, 2.4	0.2 λ_c , 0.013 λ_c
[23]	2400 (10), 5500 (6)	2.29	slots	1, 0.26	0.65 λ_c , 0.012 λ_c
[24]	3530 (12.5), 6830(4.5)	1.93	slots	4, 3.38	1.32 λ_c , 0.019 λ_c
[26]	1176 (2.5), 1227 (2.2), 1575 (1.1), 2300(2.7)	1.04, 1.34, 1.283	slots	3.4, 2.91, 2.23, 2.7	2.6 λ_c , 0.02 λ_c
[27]	2423 (5), 3381 (2), 4233 (9.5)	1.39, 1.75, 1.25	stubs, slots	7.5, 8.7, 8.7	> 5 λ_c , 0.06 λ_c
[28]	708 (3), 1053 (17), 1975 (4.7)	1.48, 2.78, 1.87	Parasitic patch	7.6, 7.2, 7.3	5.3 λ_c , 0.03 λ_c
[29]	3683 (1.57), 5910 (2.23)	1.6	slot, shorting post	10.2, 10	3.02 λ_c , 0.036 λ_c
[30]	2050 (0.5), 2750 (4), 3800 (5.5), 6500 (19.5)	1.34, 1.854, 1.382	Parasitic patch	2, 1.3, 3.1, 3.3	2 λ_c , 0.065 λ_c
[31]	1184 (2.7), 1580 (2.5)	1.334	slots	3.68, 3.31	1.92 λ_c , 0.02 λ_c

Multiband configurations reported in [8] – [9] yield lesser BW in the respective bands, although fabricated on a thicker substrate. Against this the proposed multiband configuration yields wider BW in each band. Owing to the use of metamaterial and artificial magnetic conductor (AMC) for to obtain the gain and BW enhancement, the overall complexity, cost, and volume of the configuration increases for the triple and dual-band designs reported in [10] – [12]. In spite of the AMC structure, gain offered by the antenna discussed in [10] is lower or comparable against the proposed design. In opposition to these, proposed configurations are made using a low cost FR4 substrate that is suspended in the air. The complexity of the structure for a multiband antenna mentioned in [13] to obtain a wideband response grows due to the nested integrated fractal geometry. Reconfigurable designs with active devices as discussed in [14] – [16], make the implementation challenging because of the biasing circuits. The configurations described in [18], [24] exploit a modified ground plane

structure to realize a multi-band response. But the study presented in the same does not explain how a changed ground plane produces the results that are shown, while explaining effects on the resonant modes of the patch geometry. In order to achieve dual band response, two square rings with quadrilateral feed patches are used in [21], shorting pins are used for tuning of dual band response in [22], while multiple slots are intended for the recognition of dual band response in [23]. Against these configurations, the proposed design employs a pair of rectangular slots on the ground plane and offers larger BW in each band with a higher gain. The multi-band antenna reported in [26] employs multiple stack patches with equivalent patch area. But it has lower BW and gain in respective operating bands. The triple frequency design discussed in [27] has larger patch area as it employs microstrip line fed aperture coupling technique to excite the multiple resonant modes. Further it offers lower impedance BW in respective bands against the proposed triple frequency antenna. With the overlap patches employed in the multi-band design discussed in [28], patch size is larger. The slot cut and shorting posts loaded differential fed design employing circular patch is reported for dual band response in [29]. Although it offers higher gain in the two bands, but the BW in dual bands is smaller with a higher antennas size. Further, the details about resonant modes present in the multiple shorting posts loaded circular patch that achieves dual band higher gain response are not explained. For a comparable patch area, multi-band designs discussed in [30] – [31] offers lower BW and gain in first three operational frequency bands against the proposed antenna.

In some of the reported configurations considered in the comparative analysis in Table I, designs are optimized on thinner efficient microwave substrates or presented in the higher frequency range. Because of this, they have smaller area against the proposed stacked patch designs. The selection of efficient substrates increases the cost. Against this, proposed work employs a low-cost lossy substrate in air suspended configuration thus providing a cost-effective solution. In suspended substrate designs, an effective dielectric constant approach to that of the air that leads to the patch size increment in the proposed antennas. However, in Table I comparison is also presented for reported antennas having thicker substrates. In comparison against them, antenna size in proposed antennas is smaller.

Thus, in comparison to the published work, the present study proposes a simple proximity-fed multiband stacked ring shape MSAs having a total patch area of $2.6\lambda_c$, on a substrate thickness of $0.1\lambda_c$ by using rectangular slots cut ground plane. The design offers smaller frequency ratio (≤ 1.3) between the multiple frequencies. Although the area of the proposed configurations is more than a few of the reported literature configurations, the design yields BW of 16.9 % and 18.3% in the dual-band configuration, while a BW of 16.5%, 6.9%, and 7.1% in the triple band configuration. Across the respective bands, multi-band antennas show co-polar gain in the range of 3.2 dBi to 5.7 dBi, using a low cost lossy FR4 substrate in the air-suspended configuration. The proposed antenna meets the criteria for frequency agility owing to its simple construction, improved impedance BW, gain, and

frequency ratio, and covering wireless applications like E-GSM900 /Secondary surveillance radar/aeronautical radio navigation.

V. CONCLUSIONS

The proximity-fed wideband design of stub loaded circular ring shape MSA supported via ground plane embedded with rectangular slots is proposed. The ground plane's slots and stub positions on the patch aid in optimizing the separation between the patch's degenerated TM_{01d} and TM_{01v} resonant modes to achieve the impedance BW of greater than 45%. To cater to the frequency agility applications, multi-band designs using stacked variations of circular ring shape MSAs are proposed. The dual band variation offers BW of 16.9 % and 18.3% in each band with a frequency ratio of 1:1.3. The triple band design offers 16.5%, 6.9% and 7.1% of BW in three bands with frequency ratios of 1:1.12, 1:1.13, and 1:1.17 with reference to the first band frequency. For the total patch area of $2.6\lambda_c$, and substrate thickness of $0.1\lambda_c$, both the designs offer broadside linear polarized radiation patterns through a gain of above 3 to 5 dBi, across all the bands. The proposed multi-wideband configurations are useful in frequency agile applications and are useful to cover wireless applications like E-GSM900 /Secondary surveillance radar/aeronautical radio navigation.

REFERENCES

- [1] K.L Wong, *Compact and Broadband Microstrip Antennas*, New York: John Wiley and Sons, 2002.
- [2] C. A. Balanis, *Antenna Theory: Analysis and Design*, New York: 2nd ed. John Wiley and Sons, 1997.
- [3] R. Garg R, P. Bhartia, I Bahl, *Microstrip Antenna Design Handbook*, London: Artech House, 2001.
- [4] G. Kumar, K. P. Ray, *Broadband Microstrip Antennas*, USA: Artech house, 2003.
- [5] S. V. Shynu, G. Augustin, C. K. Aanandan, P. Mohanan, K. Vasudevan, "C-shaped slot loaded reconfigurable microstrip antenna", *Electronics Letters*. vol. 42, no .6, pp. 316 - 317, 2006.
- [6] S. Liu, S. S. Qi, W. Wu, D. G. Fang, "Single layer single patch four band asymmetrical U-slot patch antenna", *IEEE Transaction on Antennas and Propagation*, vol 62, no.9, pp. 4895 – 4899, 2014.
- [7] N. N. Trong, L. Hall, C. Fumeaux, "A frequency and polarization reconfigurable stub loaded microstrip patch antenna", *IEEE Transaction on Antennas and Propagation*, vol. 63, no. 11, pp. 5235 - 5240, 2015.
- [8] N. Agrawal, A. K. Gautam, K. Rambabu, "Design and packaging of multi-polarized triple-band antenna for automotive applications", *International Journal of Electronics and Communications*, vol. 113, pp. 1 - 13, 2019.
- [9] Q. Zhong, Y. Li, H. Jiang, Y. Long, "Design of a novel dual-frequency microstrip patch antenna for WLAN applications", *IEEE Antennas and Propagation Society International Symposium*, vol. 1, pp. 277 - 280, 2004.
- [10] A. Ghosh, V. Kumar, G. Sen, S. Das, "Gain enhancement of triple-band patch antenna by using triple-band artificial magnetic conductor", *IET Microwaves. Antennas & Propagation*, vol. 12, no. 8, pp. 1400 - 1406, 2018.
- [11] C. Yu, S. Yang, Y. Chen, D. Dongdong Zeng, "Radiation enhancement for a triband microstrip antenna using an AMC reflector characterized with three zero-phases in reflection coefficient", *Journal of Electromagnetic Waves and Applications*, vol. 33, no. 14, pp. 1846 - 1859, 2019.
- [12] S. Roy, U. Chakraborty, "Metamaterial-embedded dual wideband microstrip antenna for 2.4 GHz WLAN and 8.2 GHz ITU band applications", *Waves in Random and Complex Media*, vol. 30, no. 2, pp. 193 - 207, 2018.
- [13] N. Sharma, S. S. Bhatia, "Performance enhancement of nested hexagonal ring-shaped compact multiband integrated wideband fractal antennas for wireless applications", *International Journal of RF and Microwave Computer Aided Engineering*, vol. 30, no. 3, pp. 1 - 21, 2019.
- [14] G. Upadhyay, V. S. Tripathi, "Pin-diode based switchable multiband dual feed microstrip patch antenna", *Microwave and Optical Technology Letters*, vol. 59, no. 6, pp. 1454 - 1460, 2017.
- [15] J. Kumar, B. Basu, F. A. Talukdar, A. Nandi, "Stable-multiband frequency reconfigurable antenna with improved radiation efficiency and increased number of multiband operations", *IET Microwaves Antennas and Propagation*, vol. 13, no. 5, pp. 642 - 648, 2019.
- [16] A. K. Saroj, J. A. Ansari, "A reconfigurable multiband rhombic shaped microstrip antenna for wireless smart applications", *International Journal of RF and Microwave Computer Aided Engineering*, vol. 30, no. 10, pp. 1 - 13, 2020.
- [17] M. H. Sekko, F. S. Corraera, "Penta-band antenna for global system for mobile communications/digital cellular system/personal communications service/universal mobile telecommunications system/wireless local area network operation in portable devices", *IET Microwaves Antennas and Propagation*, vol. 13, no. 7, pp. 930 - 935, 2019.

- [18] Z. Bendahmane, S. Ferouani, C. Sayah, “High Permittivity Substrate and DGS Technique for Dual-Band Star-Shape Slotted Microstrip Patch Antenna Miniaturization”, *Progress In Electromagnetics Research C*, vol. 102, pp. 163 - 174, 2020.
- [19] N. Sharma, S. S. Bhatia, “Stubs and Slits Loaded Partial Ground Plane Inspired Hexagonal Ring-Shaped Fractal Antenna for Multiband Wireless Applications Design and Measurement”, *Progress In Electromagnetics Research C*, vol. 112, pp. 91 - 111, 2021.
- [20] P. P. Singh, S. K. Sharma, “Design and Fabrication of a Triple Band Microstrip Antenna for WLAN, Satellite TV and Radar Applications”, *Progress In Electromagnetics Research C*, vol. 117, pp. 277 - 289, 2022.
- [21] B. R. Swain, A. K. Sharma, “An Investigation of Dual-Band Dual-Square Ring (DSR) Based Microstrip Antenna for WiFi/WLAN and 5G-NR Wireless Applications”, *Progress In Electromagnetics Research M*, vol. 86, pp. 17 – 26, 2019.
- [22] Amir Jafargholi, Ali Jafargholi, B. Ghalamkari, “Dual-Band Slim Microstrip Patch Antennas”, *IEEE Transactions on Antennas and Propagation*, vol. 66, no. 12, pp. 6818 - 6825, 2018.
- [23] R. Patel, T. K. Upadhyaya, “Compact Planar Dual Band Antenna for WLAN Application”, *Progress In Electromagnetics Research Letters*, vol. 70, pp. 89 - 97, 2017.
- [24] M. M. Rahman, M. S. Islam, H. Y. Wong, T. Alam, M. T. Islam, “Performance analysis of a defected ground-structured antenna loaded with stub-slot for 5G communication”, *Sensors*, vol.19, no. 11, pp. 1 - 16, 2019.
- [25] IE3D 12.1, Zeland Software, Freemont, USA, 2007.
- [26] O. P. Falade, M. Ur-Rehman, X. Yang, G. A. Safdar, C. G. Parini, X. Chen, “Design of a compact multiband circularly polarized antenna for global navigation satellite systems and 5G/B5G applications”, *International Journal of RF and Microwave Computer-Aided Engineering*, vol. 30, no. 6, pp. 1 – 13, 2020.
- [27] Q. Tan, F. C. Chen, “Triband Circularly Polarized Antenna Using a Single Patch”, *IEEE Antennas and Wireless Propagation Letters*, vol. 19, no. 12, pp. 2013 – 2017, 2020.
- [28] A. G. Ambekar, A. A. Deshmukh, “Dual Polarized Designs of Square Microstrip Antenna for GSM and LTE Applications”, *International Journal of Communication Systems*, vol. 35, no. 10, pp. 1 – 16, 2022.
- [29] Xiao Zhang, Lei Zhu, “Dual-Band High-Gain Differentially Fed Circular Patch Antenna Working in TM_{11} and TM_{12} Modes”, *IEEE Transactions on Antennas and Propagation*, vol. 66, no. 6, pp. 3160 – 3165, 2018.
- [30] S. S. Shirabadagi, V. G. Kasabegaudar, “A Planar Suspended Multiband Yagi Antenna for WLAN, LTE, and 5G Wireless Applications”, *Progress In Electromagnetics Research C*, vol. 122, pp. 141 – 151, 2022.
- [31] C. Sahana, M. Nirmala Devi, M. Jayakumar, “Dual-Band Circularly Polarized Annular Ring Patch Antenna for GPS-Aided GEO-Augmented Navigation Receivers”, *IEEE Antennas and Wireless Propagation Letters*, vol. 21, no. 9, pp. 1737 – 1741, 2022.